MECHANICAL PROPERTIES OF FRICTION STIR WELDED CARBON STEEL JOINTS – FRICTION STIR WELDING WITH AND WITHOUT TRANSFORMATION




H. Fujii[1] **L. Cui** **K. Nakata** **K. Nogi**

Joining and Welding Research Institute, Osaka University (Japan)
E-mail: [1] fujii@jwri.osaka u.ac.jp

ABSTRACT

Low temperature friction stir welding (including below A_1 point) was successful for three types of carbon steels with different carbon contents (IF steel, S12C, S35C). For all the carbon steels, the strength of the FSW joints increased when compared to that of the normal structure (ferrite + pearlite) of base metal. Compared with IF steel, the microstructures and mechanical properties of the carbon steel joints are significantly affected by the welding conditions due to the phase transformations. For the S12C steel, the welding produces a ferrite-pearlite structure, and the strength slightly increases with the increasing welding speed (decreasing the heat input) due to the refined microstructure. For the S35C steel, under the conditions exceeding the lower critical cooling rate, martensite was formed, resulting in a significantly increased joint strength; while under the conditions when martensite is not formed, the strength of the joint increased with the increasing welding speed (decreasing the heat input) due to the refined microstructures. Thus, friction stir welding enables us to control both the maximum temperature and the cooling rate in order to produce higher strength joints.

IIW-Thesaurus Keywords: *Carbon steels; Friction stir welding; Friction welding; Phase diagrams; Reference lists; Steels; Unalloyed steels.*

1 INTRODUCTION

Friction stir welding (FSW) is a solid phase welding process during which a lower heat is input to inhibit the grain growth, and therefore, it is a better welding method than fusion welding that avoids decreasing the strength of the joints [1]. Accordingly, this method has been widely investigated for mostly low melting materials, such as Al, Mg and Cu alloys [2-4]. However, the application of FSW to steels and other high temperature materials has been limited due to the absence of a suitable tool material.

Doc. IIW-1910-08 (ex-doc. III-1453r1-07) recommended for publication by Commission III "Resistance welding, solid state welding and allied joining processes".

Several previous studies [5-12] have reported the friction stir welding of carbon steels. These studies have reported that FSW achieves grain refinement in the stir zone of the carbon steel, similar to Al alloys. Additionally, a complex phase transformations also occurred during the FSW process. Accordingly, the mechanical properties were improved compared to the base metals. However, in these papers [5-8], important steel features, such as the effect of the carbon content and the transformation during the friction stir welding of the carbon steels were not systematically classified. In particular, the peak temperatures under all the welding conditions exceeded the A_3 temperature, and therefore, the effect of the phase transformation on the microstructure was not completely investigated.

Accordingly, the objective of this study is to determine the effect of the carbon content and the transformation

on the mechanical properties and microstructures of the FSW carbon steel joints. Three types of steels with various carbon contents were friction stir welded under different welding conditions. The low temperature friction stir welding of steels was also performed at around 650 °C, at which no transformation occurs.

2 EXPERIMENTAL PROCEDURE

The experiments were performed using a load-controlled FSW machine. The welding tool, which was made of a WC based material, had a 12 mm shoulder diameter, 4 mm probe diameter and 1.4 mm probe length without threads [8, 9, 13] Butt-welding of an ultra low-carbon IF steel, and two kinds of plain carbon steels with different carbon contents – JIS S12C (equivalent to UNS G10120, SAE-AIEI 1012; 0.12 wt %C) and JIS S35C (equivalent to UNS G10350, SAE-AIEI 1035; 0.34 wt%C) was performed. The plates are 1.6 mm thick, 30 mm wide and 300 mm long. The chemical composition and mechanical properties of these materials are listed in Table 1. The IF steel features a ferrite single-phase over the entire range of temperature below 910 °C, though an austenite-ferrite transformation occurs at the A3 temperature (about 910 °C). For both the S12C and S35C, the austenite-ferrite transformation occurs between A3 (about 860 °C and 800 °C, respectively) and A1 (about 723 °C), and the eutectoid reaction at A1. Therefore, S12C would show a mixture of proeutectoid ferrite and pearlite when it is slowly cooled from austenite. The volume fraction of the proeutectoid perlite is expected to be 13 %. Slowly cooled S35C would also show a ferrite + pearlite structure in which the ferrite and pearlite have nearly equal volume fractions (57 % and 43 %, respectively). The S35C steel used in this study, however, is characterized by the ferrite + globular cementite two-phase structure because spheroidized annealing was performed in order to improve the machinability.

For the IF steel, an ultrafine grained material was also prepared by the accumulative roll bonding (ARB) process in order to investigate the effect of the initial grain size on the microstrucuture and mechanical properties of the joints. For the ARB process [8, 14], two sheets were layered to make the degreased and brushed surface closely fixed to each other by clips. Roll bonding was conducted by a 50 % reduction in one pass. The roll-bonded sheet was immediately cooled in water and then cut into two pieces. To produce the ultrafine grains, this procedure was repeated 5 times for the IF steel. High angle boundaries were introduced in these materials by this method. As a result, the strength of the IF steel increased to 775 MPa.

The tool was tilted 3 degrees from the plate normal direction during FSW. The rotation speed was 400 rpm and the welding speed was varied from 100 to 400 mm/min. A K-type thermocouple was inserted into the interface of the plates and separated on the bottom surface to measure the change in temperature at the centre on the bottom surface during the FSW. Additionally, the tensile properties of each joint were evaluated using three tensile specimens cut perpendicular to the welding direction from the same joint. All tensile tests were performed using an initial strain rate of 3×10^{-4} s^{-1}. The Vickers hardness profile of the weld was measured on the cross section perpendicular to the welding direction with a 0.98 N load for 15 s. The microstructures were characterized by optical microscopy, scanning electron microscopy (SEM) and transmission electron microscopy (TEM). The metallurgical inspections were preformed on a cross section of the joint after polishing and etching with nitreagent (3 %HNO_3 + 97 %(H_2O+C_2H_5OH)). In order to clarify the crystallographic features of the microstructures, an electron back-scattering pattern (EBSP) technique was also used with a field emission type scanning electron microscope (FE-SEM) operated at 25 kV. The cross section was cut perpendicular to the welding direction and then electrolytically polished in 20 ml $HClO_4$ + 180 ml CH_3COOH solution at 248 K (–25 °C) for the EBSP analysis. The EBSD measurements were carried out using a program developed by TSL Inc. (OIM™) using a Philips XL30S SEM equipped with field emission operated at 20 kV. The planes parallel to the TD were cut from the weld and scanned by EBSD. Thin foils perpendicular to the transverse direction (TD) and parallel to the welding direction were cut from the centre of the weld and electro-polished in a 100 ml HCO_4 + 900 ml CH_3COOH solution for the TEM observations. A Hitachi H-800 microscope was operated by 200 kV. A Vickers hardness test was conducted along the TD to evaluate the hardness profiles of the centre thickness. The average grain size was determined by the mean-linear-intercept method.

Table 1 – Chemical composition and mechanical properties of carbon steel

Type	Chemical composition in mass %							Mechanical properties		
								Tensile strength	Yield strength	Elongation
	C	Si	Mn	P	S	Cu	Ti	(Mpa)	(Mpa)	(%)
IF	0.002	–	0.10	0.01	–	–	0.04	284	155	92
S12C	0.12	–	0.29	0.008	0.02	–	–	317	202	76
S35C	0.34	0.21	0.69	0.012	0.003	0.01	–	574	303	57

3 RESULTS AND DISCUSSION

3.1 Effect of welding conditions on temperature and mechanical properties

Figure 1 shows the tensile properties of the carbon steel FSW joints welded at different welding speeds. The heat input (energy input per unit weld length) decreases with the increasing welding speed at a constant rotation speed [15]. Because all the tensile specimens involving the entire joint fractured in the base metals for the sound joints [8], small tensile specimens of which the gauge length was covered by the weld nugget shown in Figure 1 a) were used to characterize the tensile properties of the stir zone. In this case, the strength of the IF steel joints slightly increased with the increasing welding speed (decreasing heat input), while the dependence of the welding speed for S12C and S35C are greater than that of the IF steel. For the S12C steel, the strength of the joints increased with the increasing welding speed (decreasing heat input), while for the S35C steel, the strength of the joints showed a peak near 200 mm/min.

Thermocouples were embedded on the bottom surface at the centreline. The peak temperatures increase with the decreasing welding speeds for all three types of steels. The heating and cooling rates of the three types of steels, on the other hand, decrease with the decreasing welding speeds. It is noted that the peak temperatures at the 400 mm/min welding speed are about 650 °C for the IF steel, S12C and S35C, which are all below A_1. It can be stated that the temperatures much lower than the peak temperatures reported in the previous papers [5-7] were controlled in this study. On the other hand, the temperature could exceed the A_1 or A_3 temperature under the conditions of a high heat input.

3.2 IF steel with a ferrite one-phase structure

Figure 2 shows an SEM image of the microstructures of the base metal. The base metal of the IF steel consists only of ferrite. Figure 3 shows the TEM bright field images of the stir zones welded at 400 mm/min. The microstructures consist of equiaxed grains including dislocations. The dislocation density seems to be higher than that in the stir zone in the FSW processed commercial purity aluminium [16]. This is caused by the restricted recovery during the FSW process due to higher melting temperature of the steel.

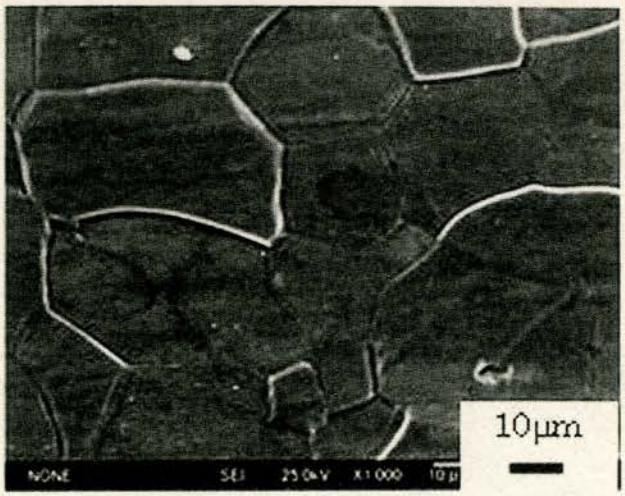

Figure 2 – SEM image of microstructure of IF steel base metal

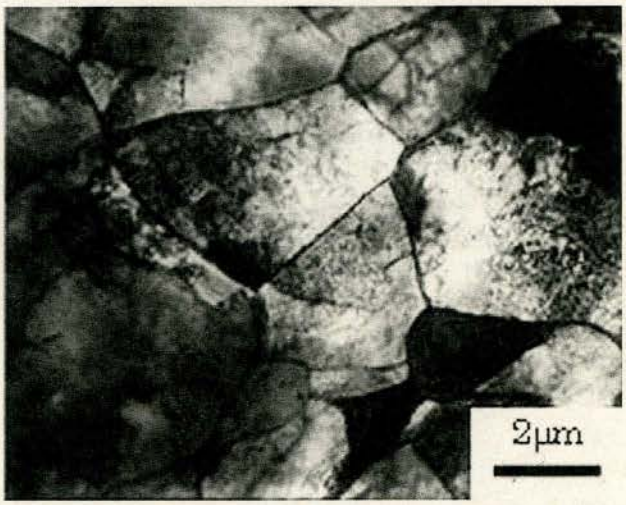

Figure 3 – TEM bright field images of stir zones of IF steel welded at 400 mm/min

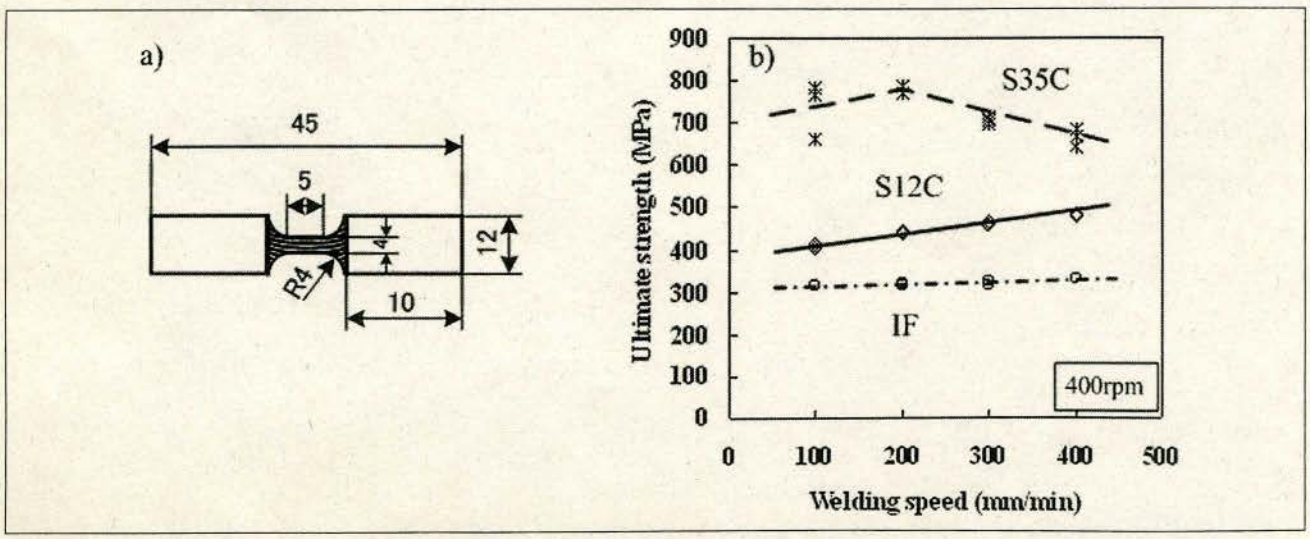

Figure 1 – Configuration and size of tensile specimens and tensile strength of FSW steel joints

It is found that the grain size at the centre of the stir zone is 5 μm at 400 mm/min, which is much smaller than that of the base metal, 24 μm. When the welding speed is 100 mm/min, the grain size is 6 μm. The bottom surface temperatures under the highest (100 mm/min) and lowest (400 mm/min) heat input conditions reached 839° C and 643 °C, respectively. It was revealed that all of the IF steels were welded in the ferrite single-phase region, and no transformation occurred. Therefore, the grain refinement is the major hardening factor of the material.

Because the grain size did not significantly decrease with the decreasing heat input, the strength only slightly increased by less than 4 %, as shown in Figure 1. Similar results are obtained for the aluminium alloys or copper alloys, etc., in which no transformation occurs during the welding, namely, the strength of the joints slightly increases with the decreasing heat input [4, 17-20].

Figure 4 shows the hardness profile of the normal grained and ultrafine grained IF steel joints welded at 400 mm/min. The hardness of the stir zone of the ultrafine grained steel joint decreased from the base material. On the other hand, the hardness of the stir zone of the normal grained steel joint increased from the base material.

Figure 5 shows TEM images of the ultrafine grained IF steel joints. Figure 5 a) shows the base material and Figure 5 b) shows the stir zone of the ultrafine grained IF steel joint welded 400 mm/min. For the ultrafine grained IF steel, the grain size of the stir zone was larger than that of the base material and the number of dislocations in the equiaxis grains is smaller than that of the base material. Consequently, the strength of the stir zone decreases. The obtained stir zone structure is similar to that for the normal grained IF steel, although the grain size of the ultrafine grained IF steel is slightly smaller. Based on these results, it is found that the strength of the FSWed IF steel joints cannot significantly be changed by the welding conditions and the initial grain size.

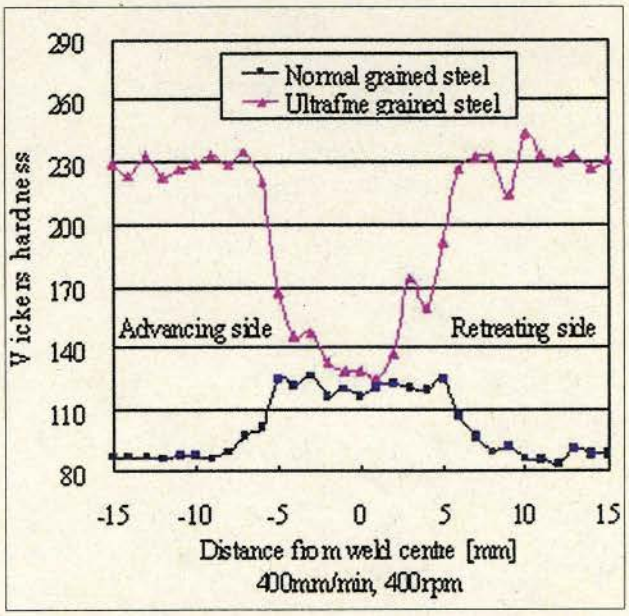

Figure 4 – Hardness profiles of IF steel joints

3.3 S12C with small proportion of pearlite

Figure 6 shows the microstructure in the stir zones of the friction stir welded joints of the S12C steel. It was found that the ferrite-pearlite structures with a limited amount of pearlite were obtained under all the welding conditions. Under the lower heat input condition (400 rpm, 400 mm/min), the bottom surface temperature was about 640 °C. In this case, FSW is performed below the A_1 temperature and therefore, the transformation does not occur during cooling after welding. Accordingly, the pearlite in the base metal was stirred and fractured into small pieces, so that the carbides were uniformly distributed in the ferrite matrix. Similarly, the breakup of constituent particles is also present in the friction stir weld of the metal matrix composites (MMC) [21, 22] and the cast Al-Si alloy [22, 23], resulting in the increased hardness of the welds.

Under the higher heat input condition (400 rpm, 100 mm/min), on the other hand, almost the entire

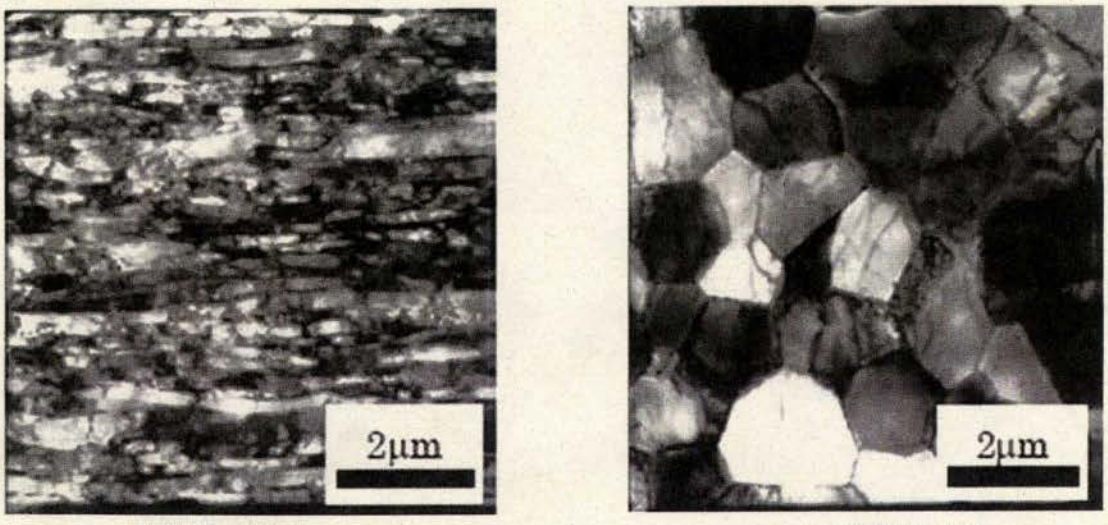

a) Base metal **b) Stir zone**

Figure 5 – Bright field images of ultrafine grained IF steel

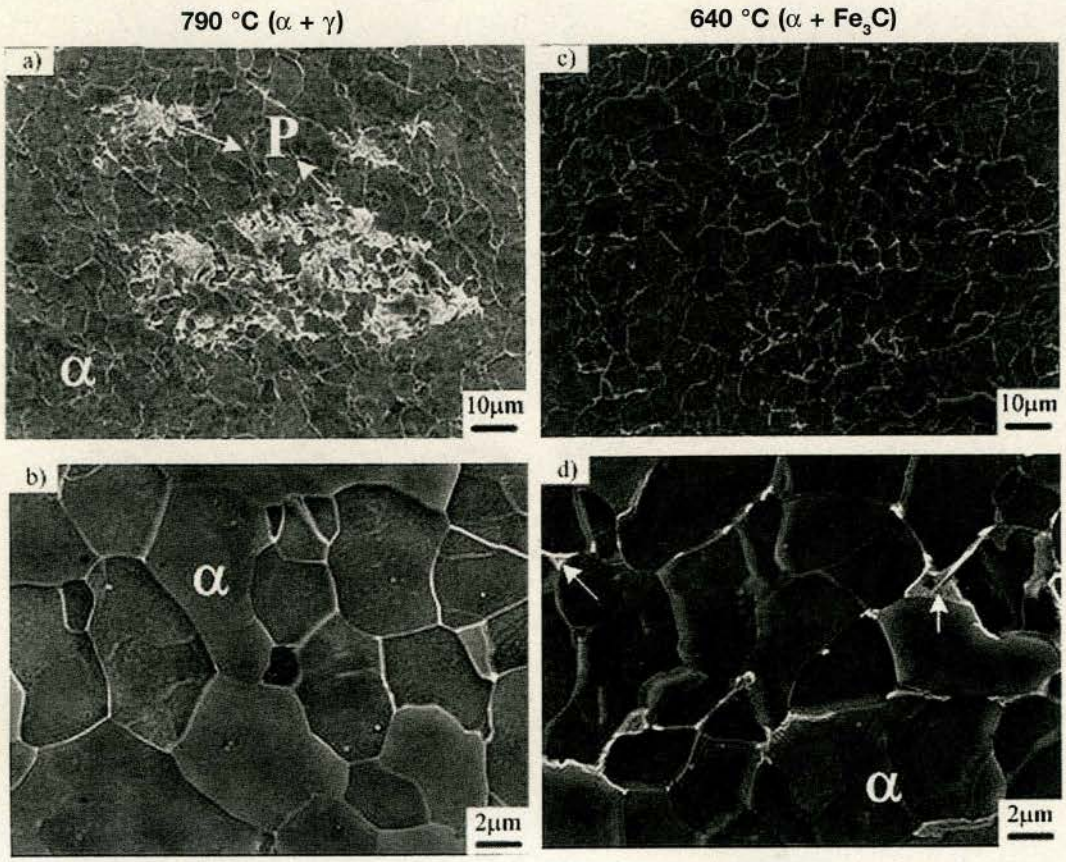

The arrows in d) indicate pearlite.

Figure 6 – SEM microstructures of the stir zone in S12C FSW joints: a), b) 400 rpm, 100 mm/min; c), d) 400 rpm, 400 mm/min

microstructure consists of equiaxed ferrite grains, while several large pearlite clusters were found in limited areas. However, under the lower heat input conditions (400 rpm, 400 mm/min), small pearlite colonies and carbides were uniformly distributed in the ferrite matrix.

The peak welding temperature measured on the bottom surface was 790 °C under the higher heat input conditions (400 rpm, 100 mm/min), which reveals that the S12C steel welding was performed in the ferrite-austenite two-phase region, and that transformation then occurred during cooling after welding. In this case, because only the austenite with a small proportion (about 13 %) was transformed into the pearlite below A_1, the pearlite distribution is not uniform. The ferrite grain size is fairly small (about 5 μm), because heavy deformation in the ferrite + austenite two-phase region causes fine recrystallized microstructures.

The area having uniformly distributed carbides increases with the increasing welding speeds, while the ferrite grain size does not significantly change. This is because the temperature near the sample surface is higher, and therefore, the area where the temperature exceeded the A_1 point decreases with the increasing welding speed.

3.4 S35C with large proportion of pearlite

Figure 7 shows the microstructures in the stir zones of the friction stir welded joints of the S35C steel. It was found that the ferrite-pearlite structures were mainly

a) 400 rpm, 100 mm/min **b) 400 rpm, 200 mm/min** **c) 400 rpm, 400 mm/min**

Figure 7 – SEM microstructures of the stir zone in S35C FSW joints

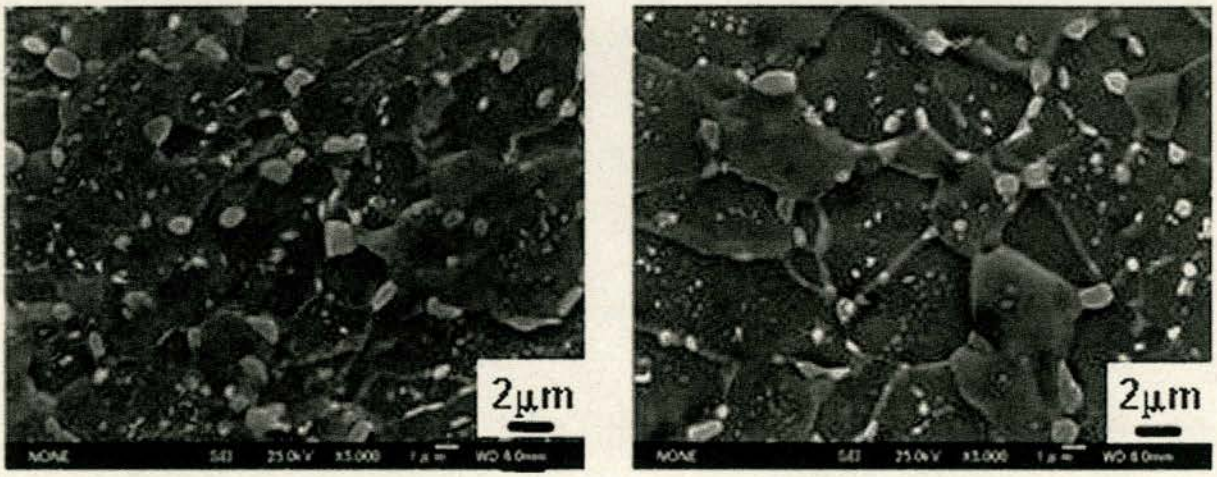

a) 400 rpm, 400 mm/min **b) Base metal**

Figure 8 – SEM microstructures of S35C near the bottom

obtained in the stir zones under almost all the welding conditions. The microstructure under the lowest heat input condition (400 rpm, 400 mm/min) shows a fine ferrite + partially deformed pearlite in the upper part, but a ferrite + globular cementite structure in the lower 1/3 part, which is similar to the base metal, as shown in Figure 8. The peak welding temperatures (on the bottom surface) at the welding speeds of 100, 200 and 400 mm/min are 873 °C, 741 °C, and 653 °C, respectively. These temperatures correspond to the austenite single-phase region, the ferrite + austenite two-phase region and the ferrite + cementite two-phase region, respectively.

Because the bottom surface temperature under the lowest heat input condition (400 rpm, 400 mm/min) of 653 °C is below A_1, the S35C steel welding was performed in the ferrite + cementite two-phase region on the bottom, and therefore, the transformation should not occur during cooling after welding. Consequently, the microstructure is almost the same as that in the base metal, as shown in Figure 8, while the ferrite grain size slightly decreased from the base metal due to the recrystallization. This result indicates that despite stirring by the tool, the microstructure was not significantly changed under this condition. However, the temperature on the upside of the stir zone seems to exceed A_1. Consequently, the partially deformed pearlite structure was formed in the upper part of the stir zone. It is deduced that, although the peak temperature slightly exceeded A_1, the temperature soon decreased to below A_1, just after the tool went through the position, but the metal is still being stirred.

Because the ferrite + globular cementite structure, which is softer than the ferrite + pearlite structure, exists in the lower part, the tensile strength of the entire weld joints decreased when the welding speed exceeded 200 mm/min, as shown in Figure 1. Under the medium heat input condition (400 rpm, 200 mm/min), the ferrite + pearlite structure is the finest and the joint strength is the highest. This is because the peak temperature was in the ferrite-austenite two-phase field.

4 SUMMARY

The effect of the carbon content and the transformation on the mechanical properties and microstructures of the FSW carbon steel joints was investigated. The low temperature friction stir welding of steels was successful at around 650 °C, at which no transformation occurs. In addition, the control of the temperature enabled the steels to be welded in various regions, such as the $\alpha + \gamma$ two-phase region and the γ single-phase region. As a result, the following conclusions were achieved.

(1) The mechanical properties of steel joints are significantly affected by the welding conditions and carbon content. Compared with the IF steel, the microstructures and mechanical properties of the carbon steel joints are significantly affected by the welding conditions. The mechanical properties of IF steel joints are not significantly changed by the welding conditions and the initial grain size.

(2) The strengths of the S12C steel joints increased with the increasing welding speed (decreasing the heat input), while the strengths of the S35C steel joints show a peak near 200 mm/min.

(3) This can be explained by the relationship between the peak temperature and the A_1 or A_3 point. When the friction stir welding is performed in the ferrite-austenite two-phase region, the microstructure is refined and the highest strength is then achieved for the S35C steel.

(4) Thus, friction stir welding enables us to control both the maximum temperature and the cooling rate and then produce higher strength joints.

ACKNOWLEDGEMENTS

The authors wish to acknowledge the financial support of the Toray Science Foundation, ISIJ Research Promotion Grant, Iketani Foundation, a Grant-in-Aid for the Cooperative Research Project of Nationwide

Joint-Use Research Institutes on Development Base of Joining Technology for New Metallic Glasses and Inorganic Materials, "Priority Assistance of the Formation of Worldwide Renowned Centers of Research - The 21st Century and global COE Programs (Project: Center of Excellence for Advanced Structural and Functional Materials Design) " from the Ministry of Education, Sports, Culture, Science and Technology of Japan and a Grant-in-Aid for Science Research from the Japan Society for Promotion of Science. The materials were provided by the JFE Steel Co., Ltd. This support is gratefully appreciated by the authors.

REFERENCES

[1] Thomas W.M., Nicholas E.D., Needham J.C., Murch M.G., Temple-Smith P., Dawes C.J., International Patent Application No. PCT/GB92/02203.

[2] Dawes C.J., Thomas W.M., Weld. J.,1996, 75, pp. 41-45.

[3] Park S.H.C., Sato Y.S., Kokawa H., Scripta Mater., 2003, 49, pp. 161-166.

[4] Park H.S., Kimura T., Murakami T., Nagano Y., Nakata K., Ushio M., Mater. Sci. Eng. A, 2004, 371, pp.160-169.

[5] Thomas W.M., Threadgill P.L., Nicholas E.D., Sci. Technol. Weld. Join., 1999, 4, pp. 365-372.

[6] Lienert T.J., Stellwag W.L., Grimmett B.B., Warke R.W., Weld. J., 2003, 82, pp.1s-9s.

[7] Reynolds A.P., Tang W., Posada M., DeLoach J., Sci. Technol. Weld. Join., 2003, 8, pp. 455-460.

[8] Fujii H., Ueji R., Takada Y., Kitahara H., Tsuji N., Nakata K., Nogi K., Mater. Trans., 2006, 47, pp. 239-242.

[9] Fujii H., Cui L., Tsuji N., Maeda M., Nakata K., Nogi K., Mater. Sci. Eng. A, 2006, 429, pp. 50-57.

[10] Ueji R., Fujii H., Cui L., Nishioka A., Kunishige K., Nogi K., Mater. Sci. Eng. A, 2006, 423, pp. 324-330.

[11] Cui L., Fujii H., Tsuji N., Nogi K., Scripta Mater., 2007, 56, pp. 637-640.

[12] Cui L., Fujii H., Tsuji N., Nakata K., Nogi K., Ikeda R., Matsushita M., ISIJ Int., 2007, 47-2, pp. 299-306.

[13] Fujii H., Cui L., Maeda M. Nogi K., Mater. Sci. Eng. A, 2006, 419, pp. 25-31.

[14] Tsuji N., Ito Y., Saito Y., Minamino Y., Scripta Mater., 2002, 47, pp. 893-899.

[15] Colegrove P.A., Shercliff H.R., Sci. Technol. of Weld. Joining, 2003, 8, pp. 360-368.

[16] Fujii H., Takada Y., Tsuji N., Nogi K., 5th Int. Symp. FSW, CD-ROM, 2004.

[17] Sato Y.S., Park S.H.C., Kokawa H., Metall. Mater. Trans. A, 2001, 32A, pp. 3033-3042.

[18] Sato Y.S., Urata M., Kokawa H., Ikeda K., Mater. Sci. Eng. A, 2003, 354, pp. 298-305.

[19] Liu H.J., Fujii H., Maeda M., Nogi K., J. Mater. Sci. Lett., 2003, 22, pp. 41-43.

[20] Liu H.J., Fujii H., Maeda M., Nogi K., J. Mater. Sci. Technol., 2004, 20, pp. 103-105.

[21] Shindo D.J., Rivera A.R., Murr L.E., J. Mater. Sci. 2002, 37, pp. 4999-5005.

[22] Liu H.J., Fujii H., Nogi K., Mater Sci. Technol., 2004, 20, pp. 399-402.

[23] Fujii H., Kim Y.G., Tsumura T., Komazaki T., Nakata K., Mater. Trans., 2006, 47, pp. 224-232.